Separation Science and Technology
Publication details, including instructions for authors and subscription information:
http://www.informaworld.com/smpp/title~content=t713708471

A Novel Technique for the Characterization of Asymmetric Membranes by Permoporometry

A. M. Vaidya[a]; N. J. Haselberger[a]
[a] DEPARTMENT OF CHEMICAL ENGINEERING, UNIVERSITY OF STRATHCLYDE, GLASGOW, SCOTLAND

To cite this Article Vaidya, A. M. and Haselberger, N. J.(1994) 'A Novel Technique for the Characterization of Asymmetric Membranes by Permoporometry', Separation Science and Technology, 29: 18, 2523 — 2531
To link to this Article: DOI: 10.1080/01496399408002206
URL: http://dx.doi.org/10.1080/01496399408002206

SEPARATION SCIENCE AND TECHNOLOGY, 29(18), pp. 2523–2531, 1994

TECHNICAL NOTE

A Novel Technique for the Characterization of Asymmetric Membranes by Permoporometry

A. M. VAIDYA* and N. J. HASELBERGER
DEPARTMENT OF CHEMICAL ENGINEERING
UNIVERSITY OF STRATHCLYDE
JAMES WEIR BUILDING, 75 MONTROSE ST, GLASGOW G1 1XJ, SCOTLAND

ABSTRACT

A modified technique for the characterization of membranes by liquid displacement permoporometry has been described. The modifications allow an estimate of the shape of a pore in an asymmetric membrane to be made. The erroneous nature of the conclusions that would be drawn if permoporometric data, obtained with a membrane with asymmetric pores, is treated under the assumption of right cylindricity has been demonstrated by means of such an analysis done on a hypothetical asymmetric membrane. While there is little error in the estimation of pore radii, the pore numbers are grossly overpredicted by a right cylindrical pore model for the membrane. The extent of this overprediction increases with the asymmetry of the membrane.

INTRODUCTION

Liquid displacement permoporometry (1) is a well-established technique for the characterization of porous membranes. The technique, first used by Bechhold et al. (2), involves the displacement of a liquid wetting the pores in the membrane by another liquid, immiscible in the former. The two liquids are chosen so as to have a low interfacial tension (3). The experimental technique involves the measurement of the flux through the membrane at incremental pressures. This is quite difficult to do since the fluxes are of the order of 10^{-9} m^3/s and the pressure increments required

* To whom correspondence should be addressed.

are correspondingly small. Capanelli et al. (4) have outlined a simpler experimental technique.

In all the published literature on the characterization of membranes using this technique, the flow through the pores from which the displacement of the liquid–liquid interface has already occurred is calculated using the Hagen–Poiseuille equation (5):

$$q = \frac{\Delta P}{l} \frac{\pi d^2}{128\mu} \tag{1}$$

and the pressure at which a pore of a given radius becomes open to flow is calculated by using the Laplace–Young (6) equation for a right cylindrical pore:

$$\Delta P_b = 4\gamma \cos \theta / d \tag{2}$$

However, as is commonly known, most modern polymeric membranes have an asymmetric pore structure (7). Consequently, a pore size and distribution estimate based on the assumption that the membrane pores are right cylindrical is likely to be of questionable veracity. In this note a technique for analyzing permoporometric data for a few other shapes of membrane pore will be outlined and examples will be given to demonstrate the erroneous nature of the conclusions that can be reached when data obtained with membranes having asymmetric pores is analyzed under the assumption of right cylindricity.

THEORY

The Laplace–Young equation in its most general form is usually written as

$$\Delta P_b = 2\gamma \left(\frac{1}{r_1} + \frac{1}{r_2} \right) \tag{3}$$

In order to determine ΔP_b for a specific pore shape, one must first obtain an expression for the two principal radii of curvature, r_1 and r_2. For an irregular pore shape this is a very daunting task. However, for any axis-symmetric pore shape the two radii of curvature are equal, and from elementary geometry and trigonometry one can easily show that the correct form of the Laplace–Young equation is

$$\Delta P_b = \frac{2\gamma \sin(\beta + \theta)}{R_n} \tag{4}$$

when the interface is displaced from the constricted end of the pore, as shown in Fig. 1. The angle β can be determined from the equation

$$\beta = \frac{\pi}{2} - \tan^{-1}(f'(0)) \qquad (5)$$

where the radius of the pore at a distance x from its opening is given by the equation

$$R = f(x) \qquad (6)$$

The solution to the laminar flow problem for a Newtonian fluid in an axis-symmetric channel with diverging walls has been obtained by Blasius (8). The solution applies to any axis-symmetric pore with a diverging cross section that can be described by an equation of the form

$$R = g(\epsilon, a, b, \ldots) \qquad (7)$$

such that the first two derivatives of the radius expression have an increasing order of dependence on a small number, ε. One practical example of such a pore shape equation is

$$R = f \exp(\epsilon x) + (R_n - f) \exp(-\epsilon x) \qquad (8)$$

For channels which can be described by such equations, the flow through the channel is given by the equation

$$q = \frac{\pi}{2} \alpha \qquad (9)$$

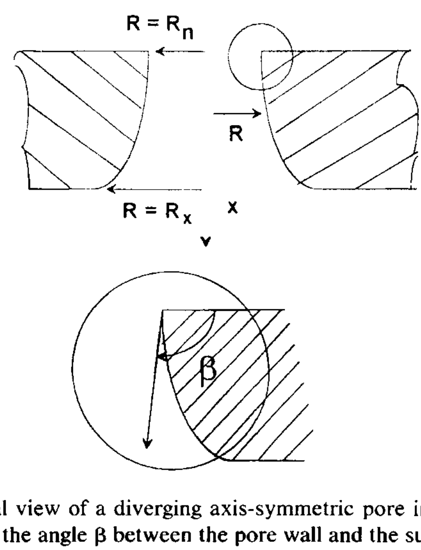

FIG. 1 Cross-sectional view of a diverging axis-symmetric pore in an asymmetric membrane. The inset shows the angle β between the pore wall and the surface of the membrane at the mouth of the pore.

α is the solution to the equation

$$E\alpha^2 + 4\mu\alpha I + \Delta P = 0 \tag{10}$$

where

$$E = \frac{1}{R_x^4} - \frac{1}{R_n^4} \tag{11}$$

and

$$I = \int_0^\lambda \frac{dx}{R^4} \tag{12}$$

The pore shape equation used must satisfy the conditions required of it by the Blasius solution to the problem of laminar flow in diverging axis-symmetric channels, as described above. However, it must also describe a pore shape which is sufficiently realistic and flexible to enable one to represent pores in a real asymmetric membrane. Equation (8) is one such pore shape. It may be considered to be a synthesis of the two extreme pore shapes described by the equations

$$R = R_n \exp(\epsilon x) \tag{13}$$

and

$$R = R_n \cosh(\epsilon x) \tag{14}$$

As can be seen from Fig. 2, Eq. (13) describes a "bell"-shaped opening—which would be too unrealistic a shape to use for the description of a membrane pore. Equation (14) describes a pore with a very small degree of asymmetry. On the other hand, Eq. (8) can be made to describe a whole family of pore shapes ranging from the bell-shaped structure of Fig. 2(A) to the virtually parallel-sided pore of Fig. 2(B). A further advantage of Eq. (8) is that the "f" term in it is constrained to obey the inequality

$$R_n/2 \leq f \leq R_n \tag{15}$$

This limitation considerably simplifies the parameter search procedure to be described in the next section. The search technique requires an independent set of permoporometric flow–pressure data for each parameter in the equation describing the pore shape. An additional data set is required to determine the number of pores. Such independent data sets can be obtained by using liquid pairs with different interfacial tensions in the permoporometric experiment. Evidently these requirements limit the utility of this modified permoporometric technique since it would be difficult to obtain more than three sets of independent flow–pressure data. For a complete analysis of pores described by Eq. (8), three data sets

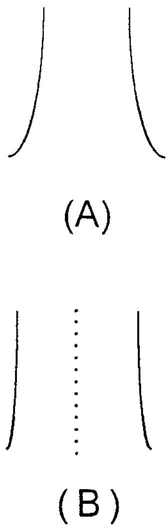

FIG. 2 Extreme examples of divergent, axis-symmetric pore shapes which meet the Blasius condition (see text). (A) A bell-shaped exponential pore. (B) A slightly asymmetric hyperbolic cosine pore.

would be required—one each for the parameters ϵ and f, and one further data set to determine the number of pores. At first sight it may appear that an additional parameter—R_n or β—must be solved for since Eq. (4) indicates that R_n is dependent on the pore angle β. However, it must be noted that one would always choose test liquid pairs in which the contact angle θ is relatively small. There is also a severe constraint on the value of the pore angle, β. It is reasonable to assume an initial value of $\pi/2$ for β. With this assumption, one can make an initial estimate to the pore size at an experimentally measured pressure ΔP by using Eq. (4) in the form

$$\Delta P_b = \frac{2\gamma}{R_n} \cos \theta \qquad (16)$$

A more refined estimate to the value of R_n can be made at a later stage after values of the pore parameters f and ϵ have been obtained.

COMPUTATIONAL TECHNIQUE

The computational technique described in this section is suitable for pore shapes given by Eq. (8). However, it can easily be adapted to obtain parameters for the other two parameter equations. The key to the technique is to note that the terms "E" and "I" in Eq. (11) are constants characteristic of the membrane pore. Consequently, if one can obtain two independent values of α, the values of E and I can be calculated by a simple Gaussian elimination method. Evidently, since the E and I values are determined by the values of R_n and R_x, both of them will be correct if, and only if, the α values used in obtaining them were correct. This suggests the following simple algorithm for the analysis of permoporometric data.

1. Read in three sets of permoporometric data obtained for the same type of membrane but with two different liquid–liquid systems. Hereafter, these data sets will be referred to as DS1, DS2, and DS3 respectively—where DS1 is obtained with the liquid pair with the lowest interfacial tension, γ, and DS3 for the liquid pair with the highest value of γ.
2. Use the first data point in DS1 to determine the radius, R_n, of the pores which will be open to flow using Eq. (4)—in the first iteration this is done with the assumption $\beta = \pi/2$.
3. From Eq. (4) obtain the opening pressure for pores with the radius calculated in Step 2 when the second liquid pair is used. Use DS2 to obtain the flow through these pores at the calculated pressure. This will have to be done by numerical interpolation if the calculated pressure is not an experimental data point.
4. Determine the α values for this pore size in the two data sets for two different guesses to the number of pores, e.g., 1 and 10^6, and at their midpoint. Using these three sets of α values, calculate three sets of values for E and I by linear elimination.
5. Repeat Steps 2 to 4 but with DS3 used in place of DS2.
6. At the end of Step 5, two sets of values for E and I are available. Compare E and I values from each set at the ends of the pore number interval used in Step 4, and reject the end of the interval which gives the greatest discrepancy in E and I. Replace the rejected end point with the midpoint of the original pore number range.
7. Repeat Steps 2 to 6 with the new pore number range. If the upper and lower limits of this range meet a preset convergence criterion, go to Step 8.
8. At this stage we have the correct values for E and I and a good estimate for the number of pores. It is necessary to use these E and I values to obtain estimates for the pore parameters f and ϵ. This process is simplified by the fact that the value of f must lie in the interval $[R_n/2, R_n]$. A bisection method—similar to the one used in the previous part of the algorithm to determine the number of pores—can hence be used. Use Eq. (8)—and the estimated value for R_n—to determine the value of ϵ when f is set to be equal to the end points of this interval.

9. For the two sets of f and ϵ values obtained in Step 8, determine the value of I from Eq. (12). Compare the two I values thus obtained with the one obtained in Step 7. Reject the end point of the interval for f which produces the largest discrepancy between these two values for I and replace it with the midpoint of the interval.

10. Return to Step 8 and repeat calculations using the new interval for f. If this interval satisfies a preset convergence criterion, go to Step 11.

11. At this stage we have estimates for the number of pores, the pore geometry parameters—f and ϵ—, and the pore radius R_n. This last value was obtained with the initial assumption $\beta = \pi/2$. Make an improved guess to the value of β using Eq. (6). Use this improved value for β and repeat Steps 1 to 10. If the value for β meets a preset convergence criterion, go to Step 12.

12. Repeat Steps 1 to 11 for all the data points in DS1.

For the purposes of illustration, a simple bisection method has been used in the algorithm described above. In an actual application, a Golden section search (9) should be employed.

EXAMPLE

It is instructive to study the results of a conventional permoporometric treatment when it is employed to analyze flow–pressure data obtained with a membrane with pores whose geometry can be described by Eq. (8). A few examples of such analyses are given in Table 1. These analyses

TABLE 1
Results of Conventional Permoporometric Analysis on a Hypothetical Asymmetric Membrane. An ϵ Value of 0.01 m^{-1} Was Assumed for the Membrane

		Calculated pore population		
Pore radius (μm)[a]	Assumed pore population	$\frac{f}{R_n - f} = 7$	$\frac{f}{R_n - f} = 4$	$\frac{f}{R_n - f} = 2$
0.7	225	261	254	242
0.6	560	650	632	601
0.5	680	789	769	730
0.4	700	814	790	753
0.3	660	765	747	709
0.2	440	518	500	475
0.1	160	466	386	287

[a] The pore sizes obtained under the assumption of right cylindricity are not significantly different from the pore sizes assumed for the hypothetical membrane.

were done by first assuming an approximately Gaussian normal distribution of pore sizes in a hypothetical membrane which has pores described by Eq. (8). Values for the parameters f and • were also assumed, and the normalized flow through each pore, α, was calculated using Eqs. (10)–(12). This α value was used in Eq. (9) along with the assumed pore number distribution to obtain an estimate of the flow through each pore—when it was available for flow. By repeating these calculations at the opening pressure for each assumed pore size, a set of flow–pressure data was obtained for this hypothetical membrane. The flow–pressure data were then analyzed using the conventional procedure as outlined by Capanelli et al. (1).

As can be seen, the discrepancy between the real pore population and the predicted one increases with the asymmetry of the pore. There is little error in the predicted value of the minimum pore radius due to the weak dependence of R_{min} on the pore angle β—for all realistic values of β. However, the conventional treatment always overpredicts the number of pores since for the same pore throat diameter the flow through a diverging pore will be greater than in the corresponding cylindrical pore.

NOMENCLATURE

d	diameter of right cylindrical pore (m)
f	pore geometry parameter for divergent pores (m)
E	a composite geometric parameter characteristic of a given size of asymmetric membrane pore (m^{-4})
I	a composite geometric parameter characteristic of a given size of asymmetric membrane pore (m^{-3})
l	length of right cylindrical pore (m)
ΔP	applied pressure (Pa)
ΔP_b	breakthrough pressure, required to move a fluid interface from a given pore (Pa)
q	flow rate of fluid through a single pore (m^3/s)
R	pore radius at a distance x from the pore mouth (m)
R_n	minimum pore radius at the pore mouth (m)
R_x	maximum pore radius (m)
r_1, r_2	principal radii of curvature of fluid interface (m)
x	axial distance from the narrow end of the membrane pore (m)
α	normalized flow rate through a single diverging pore (m^3/s)
β	angle between the membrane surface and the tangent drawn to the pore wall at the mouth of the pore (°)
ϵ	pore geometry parameter for divergent pores (m^{-1})
γ	interfacial tension at the liquid–liquid interface (N·m)

λ length of diverging membrane pore (m)
μ liquid viscosity (Pa·s)
θ angle of contact between membrane pore wall and the displaced liquid (°)

REFERENCES

1. G. Capanelli, F. Vigo, and S. Munari, *J. Membr. Sci.*, *15*, 289 (1983).
2. H. Bechhold, M. Schlesinger, and K. Silbereisen, *Kolloid. Z.*, *55*, 172 (1931).
3. F. P. Cuperus and C. A. Smolders, *Adv. Colloid Interface Sci.*, *34*, 135 (1991).
4. G. Capanelli, I. Bechhi, A. Bottino, P. Moretti, and S. Munari, in *Characterization of Porous Solids* (K. K. Unger, J. Rouquesol, K. S. W. Sing, and K. Kral, Eds.), Elsevier, Amsterdam, 1988, p. 283.
5. C. O. Bennett and J. E. Myers, *Momentum, Heat and Mass Transfer*, McGraw-Hill, Tokyo, 1982, p. 121.
6. A. W. Adamson, *Physical Chemistry of Surfaces*, Wiley–Interscience, New York, 1990, p. 8.
7. R. E. Kesting, *Synthetic Polymeric Membranes—A Structural Perspective*, Wiley, New York, 1985, p. 136.
8. H. Blasius, *Z. Math. Phys.*, p. 225 (1910).
9. W. H. Press, B. P. Flannery, S. A. Teukolsky, and W. T. Vetterling, *Numerical Recipes—The Art of Scientific Computing*, Cambridge University Press, 1988, pp. 277–282.

Received by editor March 4, 1994
Revised April 25, 1994